Available online at www.sciencedirect.com
ScienceDirect
Energy Procedia 38 (2013) 355 – 361
Energy Procedia

SiliconPV: March 25-27, 2013, Hamelin, Germany

Minimizing the optical cell-to-module losses for MWT-modules

Ingrid Haedrich[a]*, Martin Wiese[a], Benjamin Thaidigsman[a], Dirk Eberlein[a], Florian Clement[a], Ulrich Eitner[a], Ralf Preu[a], Harry Wirth[a]

[a]Fraunhofer ISE, Heidenhofstr. 2, 79110 Freiburg, Germany

Abstract

Minimizing the optical and electrical losses from cell to module is essential for highly efficient PV modules. We use metal wrap through (MWT) solar cells with passivated rear surface to integrate them into a PV-module and minimize the cell to module losses. For this purpose, we analyze the optical properties of different encapsulation materials with respect to this specific cell type, i.e. the absorption losses in the encapsulants and coupling gains from refractive index. The best performing encapsulant shows a cell-to-module power loss of 0 % for a 16-cell MWT module. The fill factor loss is 1.4 % absolute. We reach a module efficiency of 17.4 % on the aperture area implying a CTM-loss in efficiency of only 0.5 % absolute.

Keywords: CTM ratio, cell to module ratio, encapsulants, Module assembly, optical, fill factor, MWT

1. Introduction

Although the cell efficiencies increased significantly within the last years, the gains could not always be transferred to the module level. Cell to module power losses in the range of 2% to 3 % absolute can often be found on the market. The higher the efficiency of the cell the more relevant is the selection of an adequate encapsulation material. Recently the material producers introduced enhanced encapsulants with optimized optical performance. Within this work we compare different commercial and non-commercial encapsulants with respect to high-performance MWT (HIP-MWT) solar cells [1]. We characterize the

* Corresponding author. Tel.: +49-761-4588-5544; fax: +49-761-4588-9193.
E-mail address: Ingrid.Haedrich@ise.fraunhofer.de.

doi:10.1016/j.egypro.2013.07.289

optical performance of these materials to give an overview of the variation of optical losses that are related to the encapsulation.

2. Processing highly efficient solar cells

The cells used for module integration are multicrystalline HIP-MWT cells [1]. They feature a simplified structure with rear surface passivation and show an average efficiency of 18.0 %. The front side of the cells features an acidic texture, an industrial-like homogeneous emitter, a PECVD SiNx anti-reflective coating and a screen printed grid. The polished rear side with PECVD AlOx based passivation is covered by screen printed metallization and is then locally contacted by laser fired contacts (LFC). We measure the cell performances with an industrial cell tester. Table 3 shows averaged and summarized cell IV-data.

3. Optical characterization of different encapsulation materials

3.1. Interaction of optical effects within the module layers

The optical losses within a photovoltaic module have been investigated by [2] – [7]. Several optical effects have to be considered for module encapsulation. There are reflection losses at the material interfaces, mainly at the air/glass interface and on the encapsulant/cell interface. Losses from bulk absorption occur within the glass and encapsulation materials. In contrast to these optical losses there are also direct and indirect coupling gains. The direct coupling gain is due to reduced reflectance at the encapsulant/cell interface compared to air/cell interface because of better matched refractive indexes. The indirect coupling gain describes the effect of multiple reflectance's between cell surface (especially from the fingers) and the glass/air interface with subsequent total internal reflectance.

The reflectivity of the air/encapsulant interface as well as the bulk absorption can be determined from spectral measurements of transmittance (and reflectance) of a free standing material sample.

The spectral reflectance ρ and transmittance τ are measured from 317 to 2400 nm with a Fourier transform spectrometer. From this data, spectral refractive index n and bulk transmittance coefficient t are extracted using the following relationships [8] [9].

$$\tau = \frac{T_{01} \cdot T_{12} \cdot t}{1 - R_{12} \cdot R_{10} \cdot t^2} = \frac{{T_{01}}^2 \cdot t}{1 - {R_{01}}^2 \cdot t^2} \tag{1}$$

$$R_{01} = R_{10} = R_{12} = \frac{(n_1 - 1)^2}{(1 + n_1)^2} \tag{2}$$

$$T_{01} = T_{10} = T_{12} = 1 - R_{01} \tag{3}$$

$$\alpha = 1 - \tau - \rho \tag{4}$$

$$\rho = R_{01} + \frac{T_{01} \cdot t^2 \cdot R_{12} \cdot T_{10}}{1 - R_{10} \cdot R_{12} \cdot t^2} = R_{01} + \frac{{T_{01}}^2 \cdot R_{12} \cdot t^2}{1 - {R_{01}}^2 \cdot t^2} \quad (5)$$

Nomenclature

ρ	measured reflectance
T_{01}	transmittance coefficient from medium 0 (air) to medium 1
R_{01}	reflectance coefficient at the surface from medium 0 (air) to medium 1
T_{12}	transmittance coefficient from medium 1 to medium 2
t	bulk transmittance
α	absorption
n_1	refractive index of medium 1

To determine the effective absorption coefficient (α_{eff}) of glass and encapsulant, the measured values are weighted with the relative spectral response (RSR) of the cell and the solar spectrum AM 1.5.

The balance of all optical effects within a module can be determined by measuring the short circuit current of a cell against air and then comparing it to an encapsulated cell without the front glass. Subtracting the reflectance and absorption losses from the measured current differences leads to the optical coupling gain (including direct and indirect effects) [10].

3.2. Measurment setup

We investigate ten commercial and non-commercial encapsulation materials (A - K). Out of the measured transmittance and reflectance curves we calculate the refractive index *n*, the reflectance at the air/encapsulant interface R_{01} and the bulk transmittance t_{eff} (see chapter 3.3.1.).

For the electrical characterization 30 H-pattern cells with selective emitter are electrically contacted (see chapter 3.3.2.). We measure the I-V-characteristics of the contacted cells before and after encapsulation with a black backsheet and without a glass cover. For the flasher measurements a standard inline flash system with a measurement uncertainty of 3% on I_{sc} is used. The light source of the flash system emits radiation at wavelengths above 360 nm. For each type of encapsulant, three laminate samples are fabricated.

3.3. Results

3.3.1. Optical characterization

The determined optical parameters are shown in Table 1. The bulk transmittance varies between 96.8% and 99.5%. The refractive index varies between 1.41 and 1.49. An optimal encapsulant has a bulk transmittance of 100% combined with a refractive index between glass (~1.52) and the antireflective coating of the cell (~2.1). In terms of refractive index we therefore consider encapsulant K to perform best but at the same time it shows the lowest transmittance.

Table 1. Calculated bulk transmittance, surface reflectance and the refractive index weighted with the spectral response of the H-pattern solar cell with selective emitter and AM 1.5 solar spectrum

encapsulation	*A*	*B*	*C*	*D*	*E*	*F*	*G*	*H*	*I*	*J*	*K*
transmittance τ_{eff}	0,917	0,915	0,924	0,908	0,923	0,914	0,918	0,923	0,932	0,927	0,869
reflectance R_{01}	0,037	0,036	0,036	0,038	0,036	0,039	0,036	0,036	0,029	0,035	0,054
bulk transmittance t_{eff}	0,986	0,982	0,993	0,979	0,991	0,987	0,985	0,992	0,988	0,995	0,968
bulk absorption α_{eff}	0,014	0,018	0,007	0,021	0,009	0,013	0,015	0,008	0,012	0,005	0,032
refractive index n	1,47	1,47	1,47	1,48	1,47	1,49	1,47	1,47	1,41	1,46	1,61

3.3.2. Electrical characterization

The decrease of the cell current after encapsulation is given in Fig.1. The materials C, E, I, and H exhibit a decrease in current of less than 1%. Encapsulants A and B show the highest current loss, i.e. -1.9 %. It has to be considered that the measured values show a deviation of up to 0.7 % within one sample group (encapsulant C). A higher statistical confidence can only be reached by a larger amount of samples.

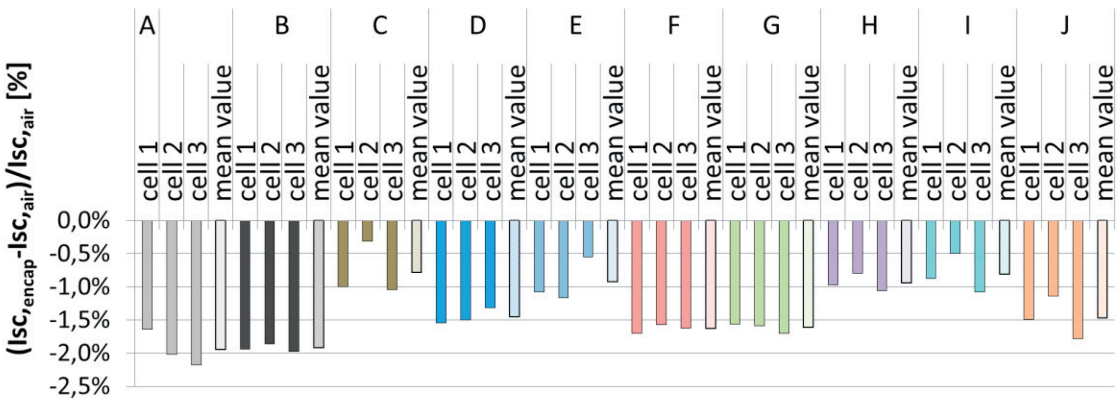

Fig. 1. Losses in short circuit current due to encapsulation in a cell/-encapsulant laminate.

Table 2: measured short circuit current initial (against air) and encapsulated without front glass and percentage difference in I_{sc} due to the embedding

Type	*Cell #*	*initial I_{sc} [A]*	*Encaps. I_{sc}[A]*	*delta I_{sc} [A]*	*Type*	*Cell*	*initial I_{sc} [A]*	*Encaps. I_{sc}[A]*	*delta I_{sc} [A]*
A	cell 1	8,84	8,69	-1,6%	F	cell 1	8,82	8,67	-1,7%
	cell 2	8,80	8,62	-2,0%		cell 2	8,78	8,64	-1,6%
	cell 3	8,88	8,69	-2,2%		cell 3	8,87	8,73	-1,6%
	mean value			-1,9%		mean value			-1,6%
B	cell 1	8,89	8,71	-1,9%	G	cell 1	8,83	8,69	-1,6%
	cell 2	8,89	8,72	-1,9%		cell 2	8,85	8,71	-1,6%
	cell 3	8,91	8,74	-2,0%		cell 3	8,86	8,71	-1,7%
	mean value			-1,9%		mean value			-1,6%
C	cell 1	8,85	8,76	-1,0%	H	cell 1	8,81	8,73	-1,0%
	cell 2	8,79	8,76	-0,3%		cell 2	8,83	8,76	-0,8%
	cell 3	8,83	8,74	-1,0%		cell 3	8,83	8,74	-1,1%
	mean value			-0,8%		mean value			-0,9%
D	cell 1	8,74	8,61	-1,5%	I	cell 1	8,85	8,77	-0,9%
	cell 2	8,74	8,61	-1,5%		cell 2	8,82	8,78	-0,5%
	cell 3	8,80	8,68	-1,3%		cell 3	8,86	8,76	-1,1%
	mean value			-1,5%		mean value			-0,8%
E	cell 1	8,86	8,76	-1,1%	J	cell 1	8,87	8,74	-1,5%
	cell 2	8,85	8,75	-1,2%		cell 2	8,84	8,74	-1,1%
	cell 3	8,80	8,76	-0,6%		cell 3	8,88	8,73	-1,8%
	mean value			-0,9%		mean value			-1,5%

4. CTM ratio for a 16 cell MWT solar module

We choose encapsulant H for encapsulating the 16 mc HIP-MWT-cells into a 4 by 4 module due to the convincing performance documented above and the good applicability for the modified lamination process for back contact solar modules.

The ribbons used for electrical interconnection exhibit a large cross-section area in order to keep the series and contact resistances low. For insulating the ribbon from the opposite polarities on the rear side of the solar cell we use a fabric embedded in the encapsulant [11]. For the backside a white highly reflective backsheet and for the front cover a 3 mm solar glass with antireflective coating is used. The string distance as well as the cell distance is 2 mm. During the module measurement a black mask is fixed on the front glass so that the cell matrix including a 1 mm wide border area is illuminated.

Table 3 shows the relevant I-V data for the solar cells as well as for the module. The cell to module ratio is calculated as relative and absolute values for every parameter. The uncertainty for the module measurement is given by 1.8% in P_{mpp}. The module efficiency is related to the aperture area defined by the mask (see above).

Table 3. Electrical parameters of multicrystalline HIP-MWT-cells measured against air in comparison to the interconnected and encapsulated 16 cell MWT module.

Cell type	V_{oc} (V)	*Isc* *(A)*	V_{mpp} *(V)*	I_{mpp} *(A)*	P_{mpp} *(W)*	*FF* (%)	η (%)
Cells measured against air	$10{,}1^{\Sigma}$	$9{,}0^{\varnothing}$	$8{,}3^{\Sigma}$	$8{,}4^{\varnothing}$	$69{,}8^{\Sigma}$	$77{,}0^{\varnothing}$	$17{,}9^{\varnothing}$
16 cell MWT module	10,1	9,2	8,1	8,6	69,8	75,6	17,4
Difference *absolute*	-0,0	0,2	-0,2	0,2	-0,0	-1,4	-0,5
Difference *relative*	-0,0%	2,3%	-2,5%	2,5%	-0,0%	-1,8%	-2,9%
Measurement uncertainty cell [%]	± 0,7	± 2,8	n.s.	n.s.	± 3,1	± 1	± 3,1
Measurement uncertainty module [%]	± 0,7	± 1,1	± 1,2	± 1,4	± 1,8	± 2,2	± 2,3

$^{\varnothing}$ mean value of measured cells, $^{\Sigma}$ Sum of measured cells

5. Conclusion

Due to our choice of the antireflective glass coating and the best matching encapsulant we are able to demonstrate a CTM-current gain in short circuit of 2.3 %. The fill factor of our MWT-module is -1.4 % (absolute) lower than the cell average. The careful analysis of the optical influences of the encapsulants and the interconnection with highly conductive material enables the excellent cell-to-module power ratio of 0 % relative. The efficiency from cell to module drops by -0.5 % absolute due to inactive areas between the cells. This investigation clearly demonstrates the potential of precise module engineering for lowest CTM-losses and highest module efficiencies.

References

[1] B. Thaidigsmann, et al. Proc. of the 26th EUPVSEC, 2011, DOI: 0.4229/26thEUPVSEC2011-2BP.1.5

[2] P. Grunow, S. Krauter. "Modelling of the Encapsulation Factors for Photovoltaic Modules," in Photovoltaic Energy Conversion, Conference Record of the 2006 IEEE 4th World Conference on, 2006, pp. 2152-2155.

[3] Y. S. Khoo. et al.. "*Method for quantifying optical parasitic absorptance loss of glass and encapsulant materials of silicon wafer based photovoltaic modules*". Solar Energy Materials and Solar Cells, vol. 102, pp. 153-158, 2012.

[4] S. Krauter and P. Grunow. "*Optical Modelling and Simulation of PV Module Encapsulation to Improve Structure and Material Properties for Maximum Energy Yield*". In: Photovoltaic Energy Conversion, Conference Record of the 2006 IEEE 4th World Conference on, 2006, pp. 2133-2137.

[5] N. E. Powell, et al., "*Improved spectral response of silicone encapsulanted photovoltaic module".* In: Photovoltaic Specialists Conference" (PVSC), 2010 35th IEEE, 2010, pp. 002791-002794.

[6] R. Preu et al.. "*PV-module reflection losses: measurement, simulation and influence on energy yield and performance ratio*". In: Proceedings of the 13th European Photovoltaic Solar Energy Conference, Nice, France, 1995, pp. 1465--

[7] McIntosh, K.R., Cotsell, J.N., Norris, A.W., Powell, N.E., Ketola, B.M.. "*An optical comparison of silicone and EVA*

encapsulants under various spectra," Photovoltaic Specialists Conference (PVSC), 2010 35th IEEE , vol., no., pp.000269,000274

[8] S. Krauter. "*Betriebsmodell der optischen, thermischen und elektrischen Eigenschaften von photovoltaischen Modulen*". In: Köster Verlag Berlin 1993. ISBN 3-929937-41-7

[9] Duffie JA, Beckman WA. "*Solar Engineering of thermal processes*". In: John Wiley & Sons: New York, USA 1991.

[10] Haedrich, I., H. Wirth, et al. (2011). "*PV Module efficiency analysis and optimization*". PV Rollout European American Solar Deployment Conference. Boston, USA.

[11] U. Eitner et al., Proc. of 27th EUPVSEC 2012, pp. 3461 – 3464